Allogenic layer silicate minerals in borehole Elmore #1, Salton Sea Geothermal Field, California

S. Douglas McDowell

Department of Geology and Geological Engineering
Michigan Technological University, Houghton, Michigan 49931

and Wilfred A. Elders

Institute of Geophysics and Planetary Physics
University of California, Riverside, California 92521

Abstract

Reaction of coarse grained allogenic layer silicate minerals with the hot, hypersaline brine of the Salton Sea Geothermal System has resulted in the formation of a series of metastable intermediate mineral phases that were created within the system, have a finite temperature range over which they exist, and react with the system in a regular but incomplete manner. Intense calcite and dolomite/ankerite cementation allowed a suite of allogenic biotite, chlorite, and muscovite grains to be preserved as unstable mineral phases to temperatures near 200°C. At this stage removal of significant portions of the cement and access of the fluid phase to these minerals initiated a series of complex reactions.

Muscovite reacted to very fine grained interlayered illite/smectite through a phengitic muscovite intermediate phase that persists in the geothermal system for less than 50°C. The overall reaction of muscovite occurred in two steps, the first involving change within the 2:1 layer via Mg addition and Al loss but little change in the interlayer sheet, and the second involving significant K loss in the interlayer site as expandable smectite layers with exchangable Mg formed. Allogenic Ti-bearing biotite reacted completely at temperatures near 200°C to a metastable optically anomalous titaniferous chlorite phase by a reaction mechanism that apparently allowed the 2:1 octahedral sheet of the reactant biotite to be preserved intact in the product chlorite. The metastable chlorite persists throughout the entire chlorite zone, shows some systematic compositional variation with temperature, but was steadily reduced in amount by reaction to fine-grained Ti-free equilibrated authigenic chlorite. At the biotite isograd at 325°C, the remaining metastable titaniferous chlorite reacted completely and rapidly to a metastable titaniferous biotite in a reaction that involved all structural sites in the minerals. This biotite reacted, within 10° above the biotite isograd, to Ti-free equilibrium authigenic biotite.

A significant degree of the compositional scatter observed in low grade metamorphic layer silicate minerals may be due to the existence of metastable mineral phases which have preserved structural elements of the mineral they originally replaced. The data suggests that some sites within minerals can remain inert while others continue to react with the fluid phase, creating partially equilibrated mineral phases and mineral reactions that must be dealt with on a site-by-site basis.

Introduction

Investigations of prograde hydrothermal metamorphism in the Salton Sea (Niland) Geothermal System have revealed a large number of systematic variations with increasing temperature in the geothermal system (Muffler and White, 1969; Helgeson, 1968; McDowell and Elders, 1980). In particular, systematic changes in authigenic layer silicate mineralogy (McDowell and Elders, 1980) with increasing temperature in borehole Elmore 1 suggest that in fine grained sandstone a significant degree of equilibration has occurred between the authigenic minerals and fluid phase in the geothermal system. It is possible to distinguish these authigenic layer silicates from a group of layer silicates that exhibit properties ranging from clearly allogenic to intermediate and ambiguous. Within this group there are numerous indications of

partial reaction with the fluid phase to form layer silicate phases that appear to be metastable with respect to the system. The purpose of this paper is to briefly discuss several examples of such metastable layer silicates and the reactions that might control their formation.

Geologic background

There exists in Elmore 1 a regular prograde zonation in sandstone from clay carbonate metamorphic facies (Zen, 1959) through chlorite and biotite zone greenschist facies to, at the base of the borehole, an andradite-garnet zone. The mineral assemblages and temperatures of these various zones are summarized in Table 1.

The gross stratigraphy of the geothermal system (Randall, 1974) consists of an upper unconsolidated to poorly consolidated clay silt-evaporite lacustrine sequence at depths shallower than approximately 350 m, and a lower moderately to well-consolidated thinly interbedded sandstone–siltstone–mudstone sequence of fluvial-deltaic origin originating from the Colorado River System (Muffler and Doe, 1968; Van de Camp, 1973). The active geothermal system is operating entirely within the deeper fluvial-deltaic sequence, while the overlying lacustrine sequence acts as a very effective stratigraphic permeability cap on that system. Within the deeper fluvial-deltaic sequence, fluid/rock interaction has resulted in a series of physical changes in the sandstones that correlate directly with the metamorphic zones. The clay-carbonate metamorphic facies consists of well-cemented low porosity sandstone

Table 1. Summary of assemblages in sandstone, Elmore 1, within fluvial-deltaic sequence. Lacustrine sequence occurs at depths of less than approximately 427 m.

|		
Carbonate cap	~185°C	depth = ~427m
	Calcite + Dolomite + mixed layer (15% exp.) + hematite(?)	
Porous Zone (chlorite grade)	190°C CHLORITE "ISOGRAD"	~439m
	Calcite + chlorite + mixed layer (0- 5% exp.) + feldspar(?) + pyrite + sphene ± anhydrite	
	243°C	~600m
	Calcite + chlorite + illite (<5% exp.) + epidote + albite + K-feldspar + quartz + pyrite + sphere ± anhydrite	
	290°C	820m
	Same as above, but illite has recrystallized to white mica or phengitic muscovite	
	325°C BIOTITE "ISOGRAD"	1135m
Hornfels Zone (biotite grade)	Biotite + quartz + epidote + K-feldspar + albite + pyrite + sphene ± talc ± vermiculite(?) + traces chlorite, muscovite, anhydrite	
	340°C	1325m
	Same as above, but actinolite appears and muscovite no longer seen	
	360°C GARNET "ISOGRAD"	2120m
Hornfels Zone (garnet grade)	Biotite + quartz + epidote + garnet + albite + actinolite + pyrite + sphene	

SALTON SEA GEOTHERMAL FIELD
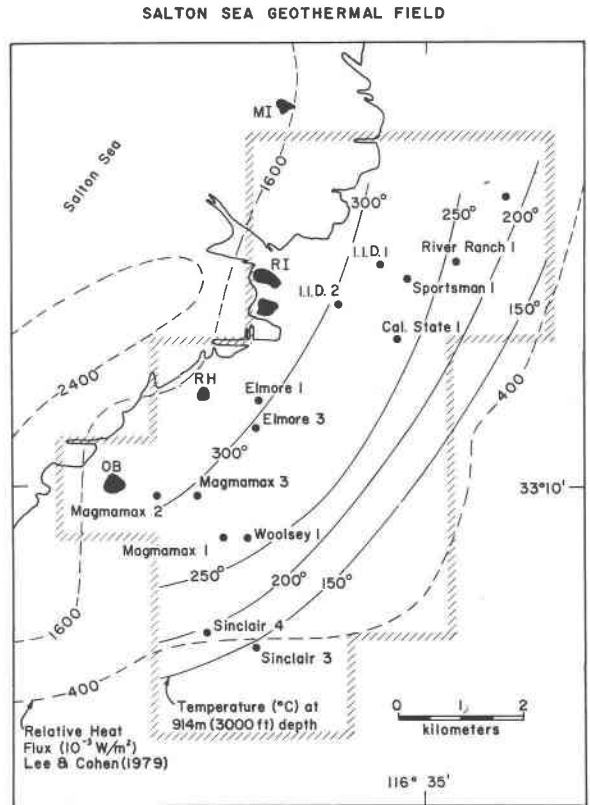
Fig. 1. Location of boreholes in Salton Sea Geothermal Field. Solid lines = temperature (°C) at 914 m (3,000 ft) depth, modified after Palmer (1975) and Randall (1974). Dashed lines = relative heat flux in 10^{-3} watts/m² from Lee and Cohen (1979). Rhyolite extrusives: OB = Obsidian Butte; RH = Rock Hill; RI = Red Island; MI = Mullet Island.

which has formed a relatively impermeable dome-shaped carbonate cap on the geothermal system entirely within the fluvial-deltaic sequence. Sandstone from the deeper chlorite zone, while still having some patchy carbonate cement, is porous and makes up the main reservoir rock in the geothermal system. The contact between the clay carbonate facies carbonate cap and the porous chlorite zone is relatively sharp and well defined in the interior portions of the geothermal field where borehole Elmore 1 is located (Figure 1). This contact, at a depth of ~439 m (190°C) in Elmore 1, represents a distinct porosity/permeability discontinuity in the geothermal system as well as defining an effective chlorite isograd. With increasing depth, sandstone porosity gradually decreases from values of 15–20% in the shallowest, lowest temperature portions of the chlorite zone to 9% in the highest temperature portions of the biotite zone where andradite garnet appears. Within the biotite zone recrystallization of both quartz and feldspar overgrowths is sufficiently intense that overgrowths are no longer commonly visible, and the sandstone has evolved into relatively low porosity hornfels.

In the shallowest, least metamorphosed sandstones that could be examined in borehole Elmore 1, a wide variety of layer silicate grains is observed ranging from pore-filling clay-sized aggregates to single grains up to 0.10 mm (rarely 0.34 mm) in length. At these depths, in sandstones completely cemented by microcrystalline to poikiloblastic carbonate cement, the distinction between the very fine-gained highly reactive authigenic clay-sized layer silicates and the coarser grained allogenic grains is clear. The allogenic layer silicates show no textural evidence of reaction to their finer grained counterparts, and have compositions consistant with a higher temperature igneous/metamorphic origin. These clearly detrital grains have apparently not been altered by the geothermal system, and have been preserved intact to temperatures up to 190°C or more in highly cemented, low porosity sandstone where no access to the fluid phase was available. X-ray diffraction investigations of the fine grained fraction of sandstones from nearby wells, which have better sample coverage within the carbonate cap, indicates that the clay fraction is continuously reacting with changing temperature in highly cemented sandstone.

Removal of the bulk of the carbonate cement at the chlorite isograd with increasing temperature and development of highly porous calcite–chlorite zone alteration has resulted in a series of reactions that affect the allogenic layer silicates. Some react directly but at variable rates to fine grained authigenic phases such as illite or chlorite which are in apparent equilibrium with the geothermal fluids (McDowell and Elders, 1980). Others react to coarse grained layer silicate minerals which are created by replacement of the allogenic layer silicates, exist over a finite range of temperatures, but react continuously to their fine grained apparently equilibrated equivalents throughout that temperature range. Such coarse grained phases are authigenic in the sense that they were created at the observed depth/temperature/fluid composition, *etc.*, but are clearly not equilibrated with the system. For want of a better term, these will be referred to as metastable phases which may represent kinetic intermediate stages in the overall reaction of coarse grained unequilibrated allogenic layer silicates to fine grained equilibrated authigenic layer silicates.

The fine grained equilibrated authigenic layer silicates progressed through a series of regular changes with increasing temperature (McDowell and Elders, 1980) that included a gradual coarsening of the originally clay-sized material to eventually produce coarser grained (up to 0.10 mm) idioblastic single crystals. The general sequence observed for the transformation of dioctahedral mica with increasing temperature starts with <0.005 mm regular mixed layer illite/smectite with about 10% expandable layers at temperatures near 190°C and progresses through <0.01 mm illite that gradually coalesces into aggregates of subparallel grains with overall dimensions approaching 0.10 mm at temperatures near 280°C. These grains appear to recrystallize into 0.10 mm clear idioblastic muscovite

grains at temperatures above 290°C. Unlike dioctahedral mica, however, both fine grained xenoblastic and coarse grained idioblastic chlorite persist to the biotite isograd at temperatures above 325°C. The textural and compositional variability of chlorite is far greater than that of white mica, reflecting the diversity of reactions that produce chlorite in sandstone. At higher temperatures, authigenic biotite also undergoes a gradual coarsening with increasing temperature.

Method of investigation

The data and observations for this paper are based mainly on petrographic examination and microprobe (mainly energy dispersive, some wavelength dispersive) analyses of layer silicate minerals in sandstone cuttings from Elmore 1. The microprobe techniques used are identical to those reported by McDowell and Elders (1980), and the reader is referred to that paper for further analytical details. The difficulties encountered due to epoxy-contamination of microprobe analyses of the fine grained authigenic layer silicate aggregates were much less prevelent on analyzing the coarser grained layer silicate minerals that are the main subject of this report.

Allogenic layer silicates

The coarse grained allogenic layer silicates in the carbonate cap sandstone consist of unreacted muscovite, chlorite and biotite which have been preserved as unstable phases to temperatures as high as 200°C. Examples of the compositions of these minerals are given in Table 2. This entire suite of minerals makes up less than 2 percent by volume of sandstone, but their relatively coarse size allows the progressive reaction of these phases to be investigated in some detail. The criteria for their identification includes various combinations of the following: (1) coarser grained, clear crystals with evidence of accumulated internal strain; (2) well developed internal cleavage reflecting a long pre-geothermal history; (3) bent and broken forms, often with splayed ends of internal separation along cleavage surfaces; (4) alteration to a variety of authigenic layer silicates; (5) compositions distinctly different from their authigenic counterpart, and characteristic of a higher temperature origin; and (6) lack of any systematic compositional change with depth/temperature in the geothermal system.

Allogenic muscovite occurs as clear, often bent or broken plates up to 0.03 mm thick and 0.10 mm long with well developed cleavage and often shadowy extinction. It is especially prevalent and is preserved to greater depths in siltstone, relative to sandstone. Its composition (Table 2,a) is distinctly different from the regular mixed layer illite/smectite (Table 3,a) stable at the boundary between carbonate cap and chlorite zone. Relative to the authigenic idioblastic coarse grained muscovite (Table 3,b) stable in the geothermal system at temperatures above 290°C, the allogenic muscovite is more sodic and contains more Fe and Mg. These characteristics suggest that the

Table 2. Allogenic layer silicates at 439 m (190°C) in completely calcite-cemented sandstone. A) Calculated assuming Σcations − Na,K,Ca = 6.00(a) or 7.00(b) or 10.00(c). B) Calculated assuming Σ + charge = 22.00 and 86.5% of $Fe_{total} = Fe^{3+}$(a) or 10% Fe^{3+}(b), or Σ + charge = 28.00 and 10% Fe^{3+}(c).

	a Muscovite	b Biotite	c Chlorite
#analyses/ #grains	7/3	17/10	3/1
A			
Si	3.07 ± 0.03	2.93 ± 0.12	2.97 ± 0.03
^{IV}Al	0.93 ± 0.03	1.07 ± 0.12	1.03 ± 0.03
^{VI}Al	1.84 ± 0.03	0.49 ± 0.18	1.23 ± 0.02
Mg	0.02 ± 0.02	1.26 ± 0.44	2.33 ± 0.02
Fe_t	0.09 ± 0.04	1.05 ± 0.31	2.33 ± 0.00
Ti	0.04 ± 0.02	0.18 ± 0.04	0.01 ± 0.01
Mn	<0.01	0.02 ± 0.01	0.03 ± 0.03
Na	0.13 ± 0.03	Trace, <0.01	0.00
K	0.84 ± 0.02	0.88 ± 0.06	0.01 ± 0.01
Ca	0.01 ± 0.01	0	0.06 ± 0.02
B			
Si	3.06	2.83	2.94
^{IV}Al	0.94	1.17	1.06
^{VI}Al	1.82	0.34	1.18
Mg	0.02	1.22	2.30
Fe^{2+}	0.01	0.92	2.08
Fe^{3+}	0.08	0.10	0.23
Ti	0.04	0.17	0.01
Mn	<0.01	0.02	0.03
ΣVI	1.98	2.77	5.83
Na	0.13	0	0.00
K	0.84	0.85	0.01
Ca	0.01	0	0.06

allogenic muscovite originated at a significantly higher temperature than did the authigenic muscovite from the geothermal system (Guidotti and Sassi, 1976).

Allogenic biotite takes the form of ragged, often bent, variably pleochroic grains up to 0.20 mm in length. Colors vary from weakly pleochroic dull green through various shades of green-brown and brown to very strongly pleochroic light brown to dark brown to red-brown. The biotite grains often have been physically disrupted by penetration of the calcite cement along cleavage planes, but there is no evidence of chemical alteration of these grains. Most biotite grains show little evidence of rounding, either by transport or alteration.

The composition of allogenic biotite (Table 2,b) is most similar to biotite from medium grade pelitic metamorphic rocks (Fig. 2) or from acid-intermediate plutonic rocks (Dodge *et al.*, 1969). The allogenic biotite at 190°C is distinctly more aluminous than the authigenic biotite (Table 3,c) that exists at ≥325°C in the geothermal system, and unlike the authigenic biotite contains a full complement of interlayer cations. The large scatter observed in allogenic biotite composition reflects the random mixing of grains originating from a variety of source

rocks and contrasts sharply with the small variability and regular compositional variation of authigenic biotite with changing temperature.

In addition allogenic biotite is distinctly titaniferous, with 0.19–0.25 Ti/3.00 octahedral cations, again contrasting sharply with the almost Ti-free authigenic biotite. The high Ti-content of allogenic biotite also supports a higher temperature origin for these biotites. The range and intensity of pleochroism in allogenic biotite increases as the Ti-content increases. The correlation of optical properties and Ti-content also holds true for reaction products of allogenic biotite deeper in the geothermal system, a fact which allows these reaction products to be traced back to their biotite progenitor.

Allogenic chlorite occurs as poorly formed grains with length:width ratios of 1.5:1 to 3:1 and typical maximum dimensions near 0.1 mm, although very rare grains up to 0.35 mm were noted. It exhibits all the textural properties of allogenic biotite in the completely cemented sandstones, and like biotite it shows no evidence of reaction to any other phase. It is, however, distinctly more rounded than biotite. In these rocks only pale green or gray-green, very weakly pleochroic chlorite grains are observed, and there is a clear optical distinction between allogenic chlorite and the more highly colored, more strongly pleochroic allogenic biotite. The allogenic biotite:chlorite ratio is approximately 2:1, while the total volume percentage of the two is seldom over 3% of any given carbonate-cemented sandstone.

The composition of allogenic chlorite (Table 2,c) from carbonate cap sandstones is grossly similar to identical appearing pale green weakly pleochroic coarse grained chlorite from the chlorite zone at higher temperatures. It is also similar to fine grained authigenic chlorite (Table 3,d), although the authigenic chlorite is texturally quite dissimilar and usually is a brighter green color very reminiscent of chrome diopside. Allogenic chlorite from the carbonate cap is Ti-poor, unlike many coarse grained chlorite grains observed in the deeper chlorite zone. The compositional overlap of coarse-grained allogenic chlorite with other chlorite types is illustrated in Figure 3.

Allogenic muscovite reaction

Unreacted allogenic muscovite is preserved only in completely calcite-cemented sandstones of the calcite cap. Alteration of muscovite starts immediately on exposure to the fluid phase as the sandstone cement is removed at temperatures >190°C, and the last identifiable allogenic muscovite is observed at 264°C (675 m depth). The only unreacted muscovite that is observed in the shallow portions of the chlorite zone occurs in patches of calcite cement preserved in sandstone. Muscovite reacts to whatever dioctahedral phase is stable at a given temperature. The lack of identifiable allogenic muscovite at higher temperatures indicates that the relatively sluggish alteration reaction was complete at these tempera-

Table 3. Authigenic, equilibrated layer silicates. A) Calculated assuming Σcations − Na,K,Ca = 6.00(a,b), 7.00(c), or 10.00(d). B) Calculated assuming Σ + charge = 22.00 and 86.5% Fe^{3+}(a,b) or 18% Fe^{3+}(c), or Σ + charge = 28.00 and 10% Fe^{3+}(d). Analyses from McDowell and Elders (1980).

	a Illite/10% Smectite 439 m (190°C)	b Idioblastic Muscovite 844.5 m (295°C)	c Biotite 1143 m (330°C)	d Chlorite 675 m (264°C)
#analyses	19	5	4	6
A				
Si	3.53 ± 0.07	3.09 ± 0.06	3.25 ± 0.05	3.10 ± 0.09
^{IV}Al	0.47 ± 0.07	0.91 ± 0.06	0.75 ± 0.05	0.90 ± 0.09
^{VI}Al	1.40 ± 0.07	1.73 ± 0.08	0.03 ± 0.02	1.58 ± 0.16
Mg	0.30 ± 0.04	0.08 ± 0.05	2.38 ± 0.09	2.23 ± 0.05
Fe_t	0.27 ± 0.04	0.16 ± 0.03	0.56 ± 0.08	2.13 ± 0.08
Ti	0.02 ± 0.02	0.02 ± 0.01	0.01 ± 0.01	0.00
Mn	0.00	0.00	0.02 ± 0.01	0.02 ± 0.02
Na	0.06 ± 0.02	0.08 ± 0.04	0.00	0.00
K	0.56 ± 0.04	0.83 ± 0.07	0.63 ± 0.03	0.02 ± 0.01
Ca	0.03 ± 0.02	0.01 ± 0.01	0.02 ± 0.01	0.02 ± 0.02
B				
Si	3.55	3.09	3.24	3.01
^{IV}Al	0.45	0.91	0.76	0.99
^{VI}Al	1.42	1.74	0.02	1.42
Mg	0.30	0.08	2.37	2.17
Fe^{2+}	0.04	0.02	0.46	1.86
Fe^{3+}	0.24	0.14	0.10	0.21
Ti	0.02	0.02	0.01	0
Mn	0	0	0.02	0.02
ΣVI	2.03	2.01	2.98	5.68
Na	0.06	0.08	0.00	0
K	0.56	0.83	0.63	0.02
Ca	0.03	0.01	0.02	0.02

tures and for the length of time necessary to reach these temperatures.

Within the lower temperature portions of the chlorite zone, allogenic muscovite exhibits a range of alteration textures on reaction to the fine grained alteration products. Where the ends of allogenic grains project into open pores, expansion and splaying of muscovite occurs. The textures so produced are almost identical to the kaolinitized white mica illustrated in Millot (1970, Plate 1, Figs. 1, 2, 5 and 6, p. 240–241). The splayed ends have often been completely replaced by aggregates of sericite-like illite grains in subparallel orientation. Partial to complete reaction rims of illite are common. In a few cases, the original muscovite has been completely replaced by a mass of illite grains in subparallel orientation with the original shape of the muscovite generally preserved.

The compositional changes resulting from alteration of muscovite to the stable dioctahedral layer silicate phase are summarized in Table 4 and Figures 4, 5, and 6. Most examples are taken from sandstone at a depth of 439 m (190°C), where an illite/smectite (I/S) with approximately 10% expandable layers is the stable authigenic phase

(McDowell and Elders, 1980). The composition of I/S which formed by complete replacement of preexisting allogenic muscovite (squares, Fig. 4 and Table 4,a) is distinctly different than the average composition of fine grained authigenic I/S (Table 3,a, and star on Fig. 4), most of which appears to have reacted continuously with increasing temperature from the original smectite-rich clay matrix. In particular I/S after muscovite contains more tetrahedral Al substitution and less octahedral Fe + Mg substitution, but similar interlayer occupancies, relative to authigenic I/S from the sandstone matrix. The distribution of authigenic matrix I/S in Figure 4 is such that most analyses cluster in an elliptical area (dashed line) around the average value, while a few analyses plot near the compositions of I/S that replaced coarse grained allogenic muscovite. It is possible that these few authigenic matrix I/S also formed by replacement of smaller allogenic muscovite grains, a reaction for which convincing textural evidence is lacking or ambiguous.

A clue to the actual reaction path followed during alteration of allogenic muscovite to authigenic I/S or illite is given in a series of analyses across a partially reacted
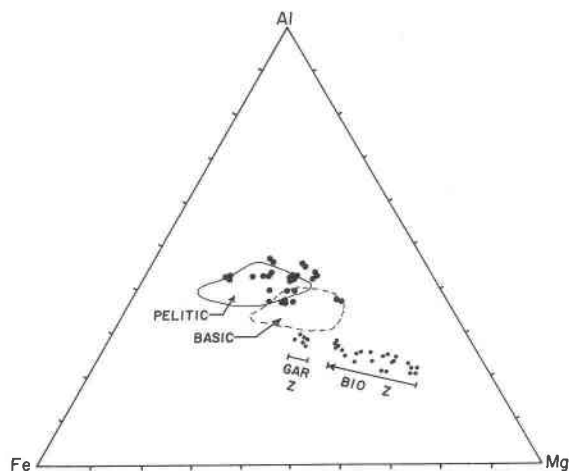
Fig. 2. Allogenic (large dots) *vs.* Authigenic (small dots) biotites in Al-total Fe–Mg system (molecular proportions). Arrows indicate change in authigenic biotite composition on increasing temperature. Area within solid line—biotites from pelitic rocks (Brown, 1967; Mather, 1970; Lambert, 1959; Chinner, 1960; Butler, 1967); within dashed line—from metabasic rocks (Cooper, 1972).

allogenic muscovite grain that shows three distinct concentric zones: (1) a clear muscovite core (Table 4,b) with uniform extinction and no evidence of alteration (x, Figs. 5 and 6); (2) a wide irregular zone (Table 4,c) which shows mottled extinction to various degrees (closed circles, Figs. 5 and 6); and (3) a thin, discontinuous outer zone (Table 4,d) consisting of an aggregate of minute, physically distinct I/S grains in subparallel orientation (open circles, Figs. 5 and 6). These zones appear to represent a progressive, stepwise replacement of muscovite by illite/smectite. The single analysis of the outermost zone approaches the composition of I/S that formed by complete replacement of another muscovite (Table 4,a).

The zonation suggests that the reaction occurs in two discrete steps. Starting with slightly phengitic allogenic muscovite, the first step in the reaction occurs entirely within the 2:1 layer of the original muscovite, with essentially no change in the interlayer position. Celadonitic substitution by Mg in the octahedral site, coupled with Si substitution in the tetrahedral site and resulting redistribution of Al, mark the major compositional changes in this step. The Fe-content remains approximately constant, resulting in a large increase in the Mg/$(Mg+Fe_t)$ ratio. Charge balance between layer and interlayer units, calculated assuming a fixed Fe^{3+}/Fe total = 0.865[1], is excellent for all analyses, and yields octahedral occupancies of 2.00 ± 0.01 in all cases. Note that an absolute loss of Al is required by this reaction.

Examination of the mottled zone at high magnifications in the petrographic microscope reveals a thin optically

[1]Average Fe^{3+} percentage of illite from analyses tabulated by Weaver and Pollard (1973).

gradational zone separating slightly larger regions or domains of variable size with relatively uniform extinction. No sharp break in optical properties is visible. The optically gradational boundary zones between domains might represent zones of lattice defect concentration that, on continuing reaction, produce true, discontinuous grain boundaries during the second reaction step when physically separable white mica grains are produced.

The formation of the optically variable defect-rich boundary zones is probably the result of lattice distortion and defect pileup during the diffusion of Si, Al, and Mg in the 2:1 layer. The resulting structurally more homogeneous domains and adjacent high energy defect zones may represent a metastable minimum energy situation which would greatly enhance the ability to move small, highly charged cations such as Al and Si within the system. True lattice diffusion would be required only to the nearest defect zone, and all further movement could take place much more rapidly through the interconnected domain boundaries and out of the original grain entirely. Note that the analyses of the mottled zone (Table 4,c) were made with an electron beam spot size (30–50 microns) considerably larger than the domains, and thus represent an average value for cations contained both within the domains and the defect-rich boundary zones. The calculated formulae in Table 4 have assumed all cations to be located within the mica structure, not in the defects, and this may not be the case in reality.

The second step in the reaction sequence involves the complete disruption of the original muscovite lattice and formation of separate I/S grains. It is during this step that most of the interlayer K is lost, while little change appears to occur within the tetrahedral site during this reaction step. The major change in interlayer K corresponds with a major change in the long range order of the crystal structure, in going from a distorted but still intact phengite to the fine grained retrograde I/S aggregate. This is analogous to the sharp prograde increase in interlayer K content observed with increasing temperature in the equilibrated authigenic phases at temperatures near 290°C in going from the fine grained illite to coarse grained idioblastic phengite (McDowell and Elders, 1980). In both
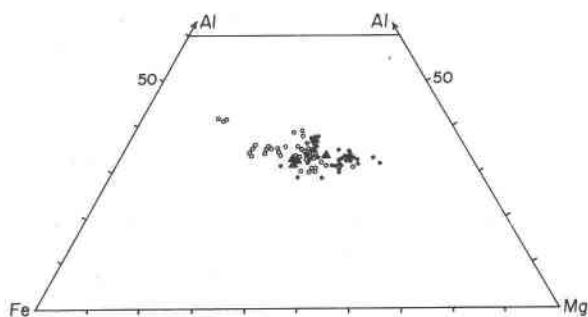

Fig. 3. Allogenic chlorite (triangles), low-Ti fine-grained chlorite (open circles), and all coarse grained high-Ti chlorite (filled circles) in Al-total Fe–Mg system (molecular proportions).
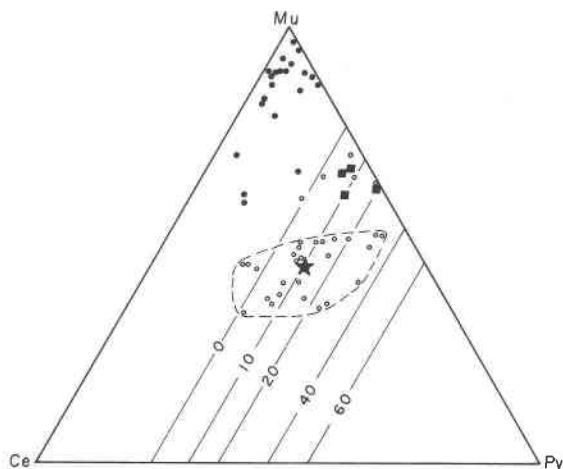
Fig. 4. Authigenic (open circles) illite/smectite, partially altered allogenic muscovite (solid circles), and allogenic muscovite completely replaced by illite/smectite from 439 m depth (190°C) (squares) plotted in Muscovite (Mu)–Celadonote (Ce)–Pyrophyllite (Py) system using method of Hower and Mowatt (1966). Unaltered muscovite plots in Mu corner (not shown). Average authigenic I/S indicated by *star*, and composition of most I/S outlined by dashed line. Contours of percent expandable layers based on data of Hower and Mowatt (1966) but drawn parallel to Mu–Ce join.

cases the major change in K content is associated with a major change in the structural integrity of the dioctahedral phase.

Note that the charge balance of the single outer illite zone analysis (Table 4,d) and the illite/smectite after muscovite analyses (Table 4,a) is very poor as calculated. If analysis 4a is recalculated assuming $Fe^{+3} = 0.865$
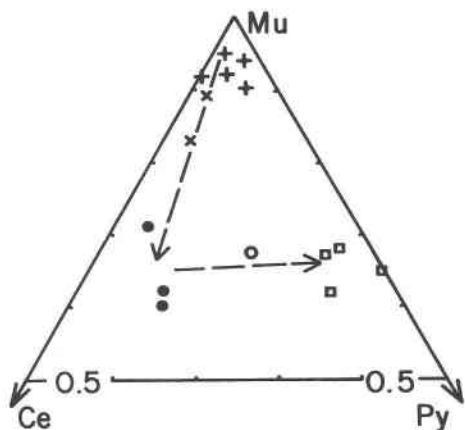

Fig. 5. Compositional changes during alteration of allogenic muscovite (plus) to authigenic illite/smectite in Muscovite (Mu)–Celadonite (Ce)–Pyrophyllite (Py) system after Hower and Mowatt (1966). Sequence of analyses from single concentrically zoned muscovite: clear muscovite core (X), mottled zone (filled circles), illitic rim (open circles). Muscovite completely replaced by illite/smectite shown by squares. Arrows indicate reaction path. 0.5 = 50% Mu. See text for details.
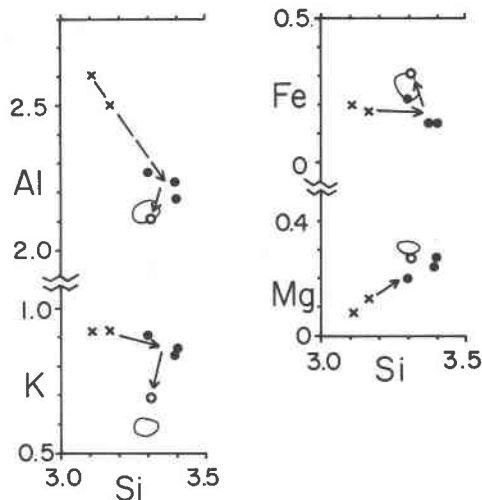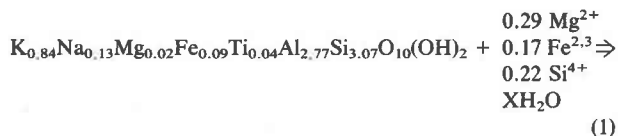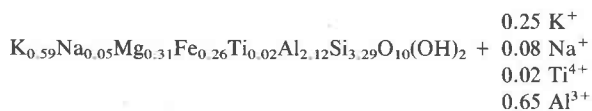

Fig. 6. Compositional changes during alteration of single concentrically zoned muscovite (formula proportions). Symbols same as in Fig. 5, except that composition of muscovite completely replaced by illite/smectite (squares in Fig. 5) indicated by area within solid line. Arrows emphasize two-step alteration sequence. Al and Fe indicate total Al and Fe, respectively. See text for details.

total Fe, and Σ+charge = 22.00, the formula becomes $(K_{0.60}Na_{0.05}Mg_{0.10})^{IL}(Ti_{0.02}Fe^{3+}_{0.23}Fe^{2+}_{0.04}Mg_{0.21}Al_{1.50})$ $^{VI}(Al_{0.66}Si_{3.34})^{IV}O_{10}(OH)_2$. The charge balance is quite good (-0.89, $+0.85$) assuming all Mg in excess of the ideal 2.00 octahedral occupancy occurs as exchangeable interlayer Mg in expandable smectite layers. Thus the second reaction steps between mottled zone and outer aggregate zone is complicated by the creation of expandable layers in this temperature range.

An overall reaction from allogenic muscovite (Table 2,a) to fine grained illite/smectite (Table 4,a) has been written below, assuming one mole of illite/smectite is produced by one mole of muscovite. Note that significant Al is lost during this reaction, and is probably consumed after moving very short distances in the fluid phase by growing authigenic phases such as chlorite, alkali feldspar, albite, or aluminous sphene. Minute chlorite grains are often observed immediately adjacent to the outer edges of allogenic muscovite grains in various stages of alteration, so that chlorite is the most plausible Al sink. If the concentrically zones grains discussed above are representative of the actual reactions, then a more realistic method of writing the overall reaction might be in the form of two steps, the first balanced assuming constant interlayer occupancy, and the second balanced assuming constant tetrahedral Si occupancy.

Allogenic Muscovite

$$K_{0.84}Na_{0.13}Mg_{0.02}Fe_{0.09}Ti_{0.04}Al_{2.77}Si_{3.07}O_{10}(OH)_2 + \begin{array}{l} 0.29\ Mg^{2+} \\ 0.17\ Fe^{2,3} \\ 0.22\ Si^{4+} \\ XH_2O \end{array} \Rightarrow$$

$$(1)$$

$$K_{0.59}Na_{0.05}Mg_{0.31}Fe_{0.26}Ti_{0.02}Al_{2.12}Si_{3.29}O_{10}(OH)_2 + \begin{matrix} 0.25 \ K^+ \\ 0.08 \ Na^+ \\ 0.02 \ Ti^{4+} \\ 0.65 \ Al^{3+} \end{matrix}$$

Replacement Illite/~10% Smectite

Alteration of allogenic biotite and chlorite

Texturally and compositionally distinct coarse grained titaniferous biotite and optically normal low-Ti chlorite make up the mafic detrital suite in the highly cemented sandstone of the carbonate cap. Chlorite is the only coarse grained mafic layer silicate observed in the calcite–chlorite zone from 622 m to the biotite isograd near 1100 m and 325°C. No coarse grained biotite is found in this interval.

Examination of sandstone cuttings at the boundary of the carbonate cap and chlorite zones at 439 m depth (190°C) indicates that all coarse grained allogenic biotite reacts very rapidly to some form of chlorite. In a few cases, alteration of highly pleochroic titaniferous biotite directly to fine grained pale green low-Ti authigenic chlorite is observed. In most cases, however, single grains of coarse grained allogenic biotite were completely replaced by single grains of chlorite (Table 5,a) through the progressive layer by layer pattern so commonly observed during retrograde alteration of biotite in metamorphic or igneous rocks. The shape, distribution and optical properties of the product chlorite grains mimic those of the reactant biotite, producing a series of optically anomalous coarse grained chlorites at the chlorite isograd. These chlorites are strongly pleochroic, with colors ranging from light yellow-brown to medium or dark brown or red brown, and birefringence as high as 0.021. As in the case of the reactant biotite, the range and intensity of pleochroic colors and the birefringence of the product chlorite increases as the Ti-content increases to a

maximum of 0.23 Ti/formula unit. The titaniferous chlorite persists through the entire calcite-chlorite zone in diminishing amounts, and everywhere within its ~135°C temperature range of existence shows evidence of reaction to fine grained low-Ti equilibrated authigenic chlorite. Thus, while authigenic, it is clearly not equilibrated but appears to be metastable with respect to the geothermal system.

The result, in the lowest temperature portions of the calcite–chlorite zone, is a series of authigenic coarse grained chlorites with highly variable optical properties ranging from optically normal pale-green weakly pleochroic grains with low birefringence to the high-Ti optically anomalous grains just described. The percentage of coarse grained authigenic chlorite is approximately equal to the combined percentage of allogenic chlorite and biotite in the adjacent carbonate cap sandstones. Since the ratio of allogenic biotite to chlorite was approximately 2:1 in the highly cemented sandstones, most of the coarse grained single chlorite crystals in the shallowest calcite–chlorite zone must have been the product of the biotite to chlorite reaction. The optically anomalous titaniferous chlorites were formed from the most titaniferous biotites, while lower titanium biotite produced more normal appearing chlorite. Much of the original allogenic chlorite from the carbonate cap persists into the chlorite zone with little recognizable reaction at the facies boundary.

Many coarse grained chlorites preserve features of a detrital origin such as bent or broken forms with splayed ends well into the chlorite zone. Shadowy extinction indicative of stored lattice strain is not observed at depths greater than 622 m (250°C), indicating some degree of internal reorganization and possible chemical exchange in these grains. The gradual coarsening of the fine grained chlorite, as well as pore filling by epidote and by quartz and feldspar overgrowths, cause features indicative of a detrital origin to gradually disappear. The titaniferous metastable chlorite remains distinctly identifiable and persists to the biotite isograd.

Relative to fine grained chlorite, coarse grained chlorite has a higher $Mg/(Mg+Fe_t)$ ratio (usually >0.5), is similar in Al-content, and may be richer in Ti if formed by reaction from allogenic biotite (Fig. 3). The compositional similarity of all chlorite types is apparent from Figure 3. The compositional scatter of chlorite appears to be strongly controlled by the specific reactant that was altered to form the authigenic chlorite, and not to variations in bulk composition or even fluid composition. Unpublished bulk chemical analyses of sandstone and shale in adjacent wells indicate relatively little compositional variation through the calcite–chlorite zone. The sandstones in this zone are very porous, and both oxygen isotope analyses (Kendall, 1976) and authigenic mineral compositions support significant fluid–rock interchange in this system. In addition, those fine grained authigenic chlorites that have replaced different allogenic phases such as alkali feldspar, plagioclase, biotite, white mica, or

Table 4. Alteration of allogenic muscovite at 439 m (190°C). All analyses calculated assuming Σcations − Na,K,Ca = 6.00. A) Muscovite completely replaced by illite/smectite. B), C), D) sequence of alteration of a single allogenic muscovite—see text for details.

	a Illite/Smectite after Muscovite 439 m (190°C)	b Clear Core	c Mottled Zone	d Outer Illite Zone
#analyses	4	2	3	1
Si	3.29 ± 0.02	3.14 ± 0.04	3.36 ± 0.06	3.31
^{IV}Al	0.71 ± 0.02	0.86 ± 0.04	0.64 ± 0.06	0.69
^{VI}Al	1.41 ± 0.04	1.69 ± 0.03	1.59 ± 0.03	1.42
Mg	0.31 ± 0.01	0.10 ± 0.04	0.24 ± 0.04	0.27
Fe_t	0.26 ± 0.03	0.19 ± 0.01	0.16 ± 0.05	0.31
Ti	0.02 ± 0.01	0.02 ± 0.00	0.01 ± 0.01	0.01
Mn	Trace	Trace	Trace	0
Na	0.05 ± 0.02	0.05 ± 0.02	0.02 ± 0.01	0.09
K	0.59 ± 0.02	0.92 ± 0.01	0.87 ± 0.04	0.69
Ca	0.02 ± 0.01	0.01 ± 0.01	0.01 ± 0.00	0.01

Table 5. Coarse grained chlorite and biotite. A) Calculated assuming Σcations − Na,K,Ca = 10.00(a) or 7.00(b,c). B) Calculated assuming Σ + charge = 28.00 and 10% Fe^{+3}(a), or Σ + charge = 22.00 and 18% Fe(b,c). Compare (c) with Table 3-c authigenic biotite.

	a Metastable Coarse Grained Ti-Chlorite 675 m (264°C)	b Metastable Coarse Grained Ti-Biotite 1143 m (330°C)	c Stable Coarse Grained Ti-Free Biotite 1143 m (330°C)
#analyses/ #grains	6/3	5/2	5/4
A			
Si	3.06 ± 0.05	2.91 ± 0.05	3.19 ± 0.05
^{IV}Al	0.94 ± 0.05	1.09 ± 0.05	0.81 ± 0.05
^{VI}Al	1.31 ± 0.14	0.47 ± 0.08	0.04 ± 0.02
Mg	2.33 ± 0.08	1.36 ± 0.13	2.33 ± 0.09
Fe_t	2.12 ± 0.13	0.99 ± 0.06	0.61 ± 0.08
Ti	0.17 ± 0.05	0.15 ± 0.01	0.01 ± 0.01
Mn	0.04 ± 0.01	0.03 ± 0.01	0.01 ± 0.01
Na	0.00	0.00	0.00
K	0.03 ± 0.01	0.80 ± 0.02	0.64 ± 0.03
Ca	0.00	0.00	0.00
B			
Si	2.97	2.83	3.19
^{IV}Al	1.03	1.17	0.81
^{VI}Al	1.15	0.36	0.04
Mg	2.26	1.31	2.33
Fe^{2+}	1.85	0.77	0.50
Fe^{3+}	0.21	0.17	0.11
Ti	0.17	0.15	0.01
Mn	0.04	0.03	0.01
ΣVI	5.68	2.79	3.00
Na	0	0	0.00
K	0.03	0.78	0.64
Ca	0	0	0.00

other chlorite have differing compositions, reflecting the strong control of the chlorite precursor in the final chlorite chemistry. Much of the large compositional scatter observed in most low grade chlorite from regional and burial metamorphic terrains may be due to similar variations in the origin of individual chlorite grains.

The compositional variation of fine and coarse grained authigenic chlorite from calcite–chlorite zone sandstones is shown in Figure 7 as a function of temperature. Compared to other authigenic minerals, the compositional variation of chlorite with temperature is very weak. However, all authigenic chlorite shows the same slight decrease in octahedral Al, increase in total Mg + Fe_t, and increase in octahedral occupancy, with increasing temperature. Thus authigenic chlorite, whether the coarse or fine grained optically normal varieties, or the coarse grained metastable titaniferous variety, appears to be responding in a systematic way to the change in depth or temperature through the calcite–chlorite zone. In particular, the metastable titaniferous chlorite, formed by direct replacement of allogenic biotite at the carbonate-cap/ chlorite zone boundary, also appears to react at least in part with the fluid phase, at the same time it reacts to the apparently stable equilibrated fine grained low-Ti authigenic chlorite. Thus the metastable chlorite that was created within the geothermal system appears to respond to temperature changes within the system, yet continu-
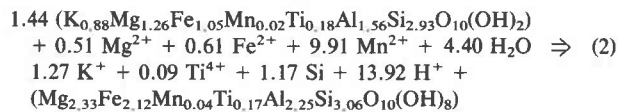
ously reacts with that system to produce an apparently stable, equilibrated chlorite variety.

Biotite/chlorite reaction near the carbonate-cap/ chlorite zone boundary

The majority of the titaniferous allogenic biotite appears to react to fine grained equilibrated chlorite in two distinct steps: (1) rapid reaction at the zonal boundary to a metastable, optically anomalous coarse grained titaniferous chlorite; and (2) sluggish reaction of the metastable chlorite to fine grained equilibrated authigenic chlorite throughout the calcite–chlorite zone.

There is a strong correlation between the development of secondary porosity and the progress of the first reaction. Sandstones from which most of the calcite has been removed contain only traces of the original biotite, which itself was preserved as an unstable phase to temperatures near 190°C by lack of fluid access in the highly cemented rocks. By using the average allogenic biotite (Table 2) and titaniferous metastable chlorite (Table 5a) analyses, it is possible to write an aluminum conservative version of the first reaction as follows:

Allogenic Biotite

$$1.44\,(K_{0.88}Mg_{1.26}Fe_{1.05}Mn_{0.02}Ti_{0.18}Al_{1.56}Si_{2.93}O_{10}(OH)_2)$$
$$+\ 0.51\ Mg^{2+} + 0.61\ Fe^{2+} + 9.91\ Mn^{2+} + 4.40\ H_2O \Rightarrow \quad (2)$$
$$1.27\ K^+ + 0.09\ Ti^{4+} + 1.17\ Si + 13.92\ H^+ +$$
$$(Mg_{2.33}Fe_{2.12}Mn_{0.04}Ti_{0.17}Al_{2.25}Si_{3.06}O_{10}(OH)_8)$$

Metastable Chlorite

The critical characteristic of the metastable chlorite is its high content of the small, highly charged titanium ion, an element that is immobile in most fluid systems. The creation of a metastable phase whose Ti-content appears to reflect that of the reactant biotite implies that specific structural elements present in the biotite are passed on to the product chlorite during the layer-by-layer replace-
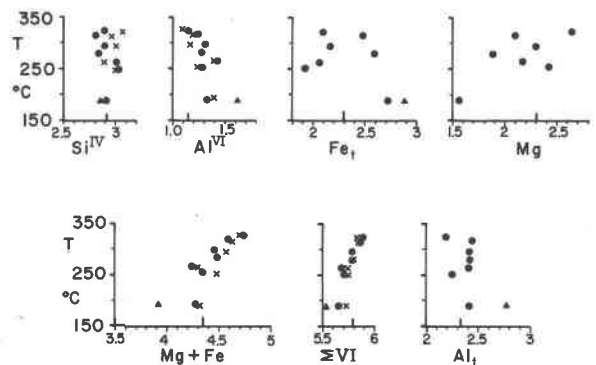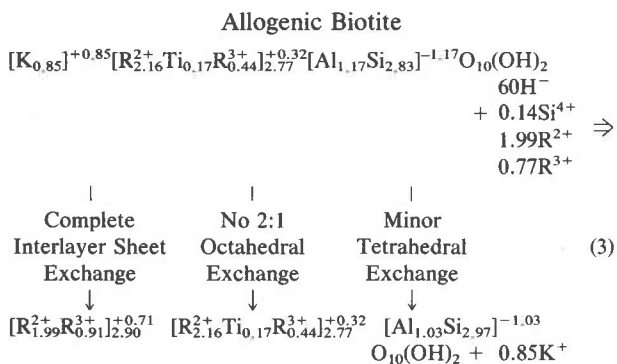

Fig. 7. Composition variation of average fine grained (solid circles) and coarse grained (X) authigenic chlorite from chlorite zone as a function of borehole temperatures (°C) (formula proportions). Bar indicates average composition of allogenic chlorite. Triangle represents average authigenic chlorite from dolomite-hematite-bearing sandstone. VI = total octahedral occupancy assuming Σ + charge = 28.00 and 10% ferric iron.

ment process. An alternative to the above reaction is to assume that the titanium stabilizes the octahedral sheet of the biotite 2:1 layer, passing on this sheet intact to the product metastable chlorite and thus allowing that metastable phase to be created and persist in the geothermal system. A hypothetical alternative reaction written using mineral formulae calculated assuming that 10% of the total Fe is ferric, and combining $Fe^{2+} + Mg + Mn$ as R^{2+} and Fe^{3+} + octahedral Al as R^{3+} is as follows:

Allogenic Biotite

$$[K_{0.85}]^{+0.85}[R^{2+}_{2.16}Ti_{0.17}R^{3+}_{0.44}]^{+0.32}_{2.77}[Al_{1.17}Si_{2.83}]^{-1.17}O_{10}(OH)_2$$

$$\begin{matrix} 60H^- \\ + 0.14Si^{4+} \\ 1.99R^{2+} \\ 0.77R^{3+} \end{matrix} \Rightarrow$$

Complete Interlayer Sheet Exchange	No 2:1 Octahedral Exchange	Minor Tetrahedral Exchange	(3)
↓	↓	↓	

$$[R^{2+}_{1.99}R^{3+}_{0.91}]^{+0.71}_{2.90} \quad [R^{2+}_{2.16}Ti_{0.17}R^{3+}_{0.44}]^{+0.32}_{2.77} \quad [Al_{1.03}Si_{2.97}]^{-1.03}$$
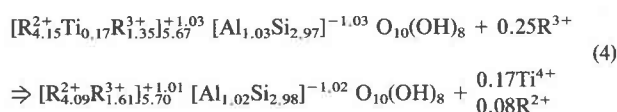$$O_{10}(OH)_2 + 0.85K^+$$

Metastable Ti-Chlorite

The gain in R^{3+} (mainly Al) is easily accounted for due to the local Al mobility in the geothermally altered sandstone required to form newly nucleated albite, orthoclase, epidote and other authigenic phases. In particular, a major Al source is represented by the absolute decrease in the authigenic illite and muscovite content on increasing temperature in these rocks. The product chlorite has a brucite-like interlayer sheet with approximately one third of the filled sites occupied by Al, a value close to the maximum observed in chlorite (Deer *et al.*, 1962). Changes in the interlayer site are balanced by changes in the tetrahedral sheet of the 2:1 layer packet, while the octahedral sheet remains constant. The R^{2+}/R^{3+} ratios in interlayer and octahedral sheets are distinctly different, and this along with the Ti-stabilized 2:1 octahedral sheet, may cause the slow but gradual breakdown of the metastable chlorite to equilibrated chlorite.

The continuous reaction of the metastable Ti-chlorite to Ti-free equilibrated chlorite implies complete exchange of the Ti-stabilized 2:1 octahedral sheet and recrystallization of a large single grain into an aggregate of small grains. Since the 2:1 octahedral sheet does not maintain its integrity, and thus there is no clear criteria for partitioning cations among the two octahedral sheets in the product chlorite, the reaction has been written by combining octahedral sheets as follows:

Metastable Ti-Chlorite

$$[R^{2+}_{4.15}Ti_{0.17}R^{3+}_{1.35}]^{+1.03}_{5.67}[Al_{1.03}Si_{2.97}]^{-1.03}O_{10}(OH)_8 + 0.25R^{3+}$$

$$\Rightarrow [R^{2+}_{4.09}R^{3+}_{1.61}]^{+1.01}_{5.70}[Al_{1.02}Si_{2.98}]^{-1.02}O_{10}(OH)_8 + \begin{matrix} 0.17Ti^{4+} \\ 0.08R^{2+} \end{matrix}$$

(4)

Equilibrated Chlorite

The reaction as written requires essentially no change in the tetrahedral site and little variation in the number of probable octahedral vacancies. Again the needed Al could be provided by the on-going continuous reaction of dioctahedral mica, while the immediate sink for the Ti produced is authigenic sphene.

Metastable chlorite/biotite reactions near the biotite isograd

Despite the continuous progressive alteration of metastable titaniferous chlorite, small amounts of it are preserved to the biotite isograd. The morphology of such chlorite is still distinct in that it maintains its ragged appearance and irregular form, in contrast to the much more idiomorphic, low-Ti chlorite which by these temperatures has coarsened considerably. The metastable chlorite is internally much more irregular, showing variable optical extinction and mottling of pleochroic colors, while the idioblastic chlorite is clear, and shows light, uniform colors, minor pleochroism, and uniform extinction.

At the biotite isograd, almost all chlorite reacts directly to biotite. The light green low-Ti idioblastic chlorite reacts to a morphologically identical light green Mg-rich biotite. This biotite is compositionally identical to the blocky <0.02 mm pale green weakly pleochroic authigenic biotite that nucleates in pore spaces at the biotite isograd (Table 3,c). The compositional uniformity of both newly nucleated biotite and biotite after idioblastic low-Ti chlorite (Table 5,c) strongly indicates complete equilibration with the fluid phase. These biotites show no evidence of reaction to any other phase at a given temperature. With increasing temperature, however, these biotites undergo a series of very regular compositional changes with temperature (McDowell and Elders, 1980) as they gradually make the transition from a siliceous, interlayer deficient biotite at the biotite isograd (325°C) to a compositionally typical greenschist facies metamorphic biotite at the garnet isograd (360°C).

The metastable Ti-chlorite does not react directly to equilibrated low-Ti biotite. Instead it reacts to an idioblastic to sub-idioblastic titaniferous, strongly pleochroic biotite with colors ranging to deep green-brown, brown-green, or brown and birefringence up to 0.040. This titaniferous biotite is also apparently metastable, as it is immediately replaced by fine grained pale green low-Ti equilibrated biotite. In the 1140–1146 m depth interval where authigenic biotite first appears, almost all of the metastable titaniferous biotite shows some evidence of reaction to equilibrated biotite, and in a few instances grains almost completely replaced by equilibrated biotite aggregates were noted. In the next deeper sampled interval at 1213–1219 m depth (~335°C) coarse grained titaniferous biotite is very rare, and the few grains that are observed are almost completely replaced by equilibrated

authigenic biotite. No evidence of the metastable Ti-biotite is observed at greater depth. Thus metastable authigenic titaniferous chlorite, which originally formed by the rapid replacement of unstable allogenic biotite at the chlorite isograd near 190°C, is itself replaced at the biotite isograd at 325°C by a metastable authiferous biotite that is in turn completely altered to stable authigenic biotite within about 10° of the biotite isograd.

Average analyses of metastable Ti-rich and equilibrated Ti-free biotite have been listed in Table 5. Unlike the original allogenic biotite or metastable chlorite, the coarse grained biotite from the biotite isograd shows very regular cation substitutions which span the gap between the broad compositional field of the original allogenic biotite and the very restricted range of equilibrated authigenic biotite compositions from the same depth (Fig. 8). The contrast between the compositional scatter of allogenic biotite, and the very restricted compositional range of the Ti-rich metastable biotite, is especially marked.

There is a regular increase in Ti-content in the coarse grained biotite from K- and Al-poor, Mg-rich grains (Table 5,c) identical in composition to fine grained equilibrated biotite (Table 3,c) to K- and Al-rich, Mg-poor grains that are very similar to the average composition of the original allogenic biotite. As Ti increases, Si, Mg+Fe$_t$ and Mg/(Mg+Fe$_t$) decreases while ^{IV}Al, ^{VI}Al, K, and Al/Al + Fe$_t$ + Mg increase in a very regular way. The most Ti-rich metastable grains, however, still have low interlayer occupancies more similar to authigenic than allogenic biotite. The Ti substitution scheme within the coarse grained sub-idioblastic biotite is very complex, and can be generalized as follows:

$$Ti^{4+} + 5R^{3+} + K^+ + 1.5^{VI}Vac.° = 2.5Si^{4+} + 5R^{2+} + {}^{IL}vac.° \quad (5)$$
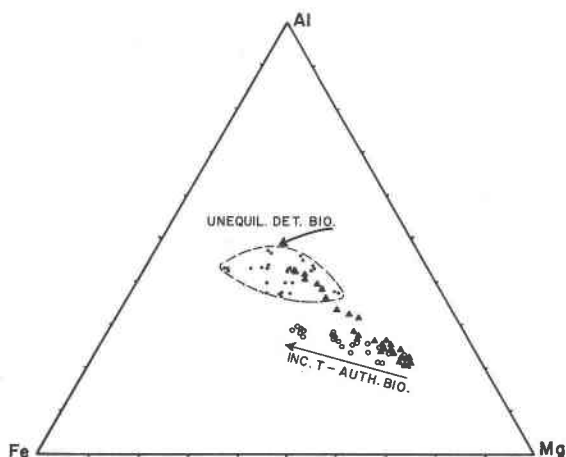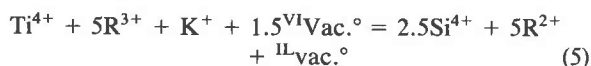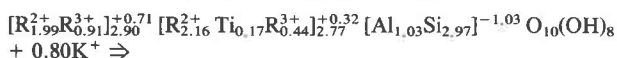

Fig. 8. Comparison of composition of allogenic biotite (filled circles), Low-Ti authigenic biotite (open circles), and metastable (triangles) Ti-biotite that exists just above 325°C only, in Al-total Fe–Mg system (molecular proportions). Compositional trend of authigenic biotite on increasing temperature indicated by arrow.
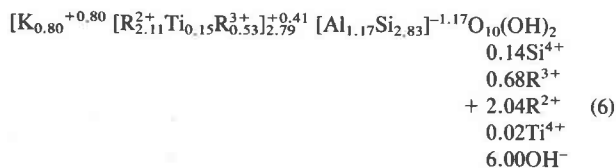
The data strongly indicates that those titaniferous coarse grained metastable chlorite grains that had not yet reacted to fine grained Ti-free equilibrated chlorite in the chlorite zone by the time temperatures reached 325°C, reacted very rapidly at that temperature to produce a metastable coarse grained sub-idioblastic titaniferous biotite. The most titaniferous chlorite produced a homogeneous titaniferous biotite very similar to the average composition of allogenic biotite that had ceased to exist at temperatures some 125°C lower than the biotite isograd. Other chlorite grains of varying Ti-contents in turn were replaced by a suite of metastable biotites with very regular intergrain compositional variations. All coarse grained xenoblastic chlorite grains that originated by reaction from original allogenic biotite were completely replaced at the biotite isograd by metastable coarse grained biotite. Those few idioblastic coarse grained chlorite grains that formed by recrystallization of fine grained equilibrated chlorite in the deeper parts of the chlorite zone did not react at the biotite isograd, but persist in trace amounts well into the biotite zone.

The reaction of metastable chlorite to metastable biotite at the biotite isograd show some critical differences relative to the reaction which originally formed the chlorite. In particular, the metastable biotite is distinctly more idioblastic than the chlorite it replaces, and is internally optically homogeneous. It shows none of the intracrystalline color and extinction variations so common in the more xenoblastic metastable chlorite, even though the intense pleochroic colors and high birefringence of the chlorite are mimiced in the product biotite. In addition, the compositional range of the metastable biotite is very restricted compared with that of the reactant chlorite. It thus appears that, unlike the chlorite isograd reaction where specific structural elements of the biotite could have been passed onto the product chlorite, at the biotite isograd the reaction of metastable chlorite to metastable biotite involves the complete recrystallization and structural reorganization of the product biotite. The titaniferous 2:1 octahedral sheet that is postulated to have allowed the metastable chlorite to persist through the calcite-chlorite zone probably was finally disrupted at the biotite isograd. Once this "stabilizing" 2:1 sheet was removed, the metastable biotite reacted relatively rapidly to equilibrated biotite.
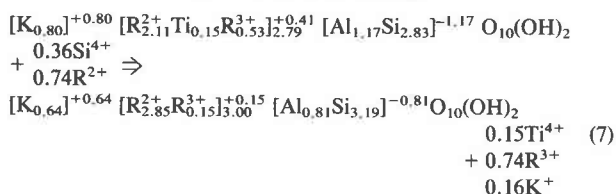
The reaction of metastable titaniferous chlorite to metastable titaniferous biotite at the biotite isograd, and of that biotite to Ti-free biotite at temperatures just above the biotite isograd are given below, using the same cation combination procedures as in previous reactions. Note that the biotites have been calculated assuming that 18 percent of total Fe is ferric after McDowell and Elders (1980).

Metastable Ti-Chlorite

$$[R^{2+}_{1.99}R^{3+}_{0.91}]^{+0.71}_{2.90} [R^{2+}_{2.16} Ti_{0.17}R^{3+}_{0.44}]^{+0.32}_{2.77} [Al_{1.03}Si_{2.97}]^{-1.03} O_{10}(OH)_8 + 0.80K^+ \Rightarrow$$

$[K_{0.80}]^{+0.80} [R^{2+}_{2.11}Ti_{0.15}R^{3+}_{0.53}]^{+0.41}_{2.79} [Al_{1.17}Si_{2.83}]^{-1.17}O_{10}(OH)_2$

$$
\begin{aligned}
& 0.14Si^{4+} \\
& 0.68R^{3+} \\
+ & 2.04R^{2+} \quad (6) \\
& 0.02Ti^{4+} \\
& 6.00OH^-
\end{aligned}
$$

Metastable Ti-Biotite

$[K_{0.80}]^{+0.80} [R^{2+}_{2.11}Ti_{0.15}R^{3+}_{0.53}]^{+0.41}_{2.79} [Al_{1.17}Si_{2.83}]^{-1.17} O_{10}(OH)_2$

$+ \begin{aligned} & 0.36Si^{4+} \\ & 0.74R^{2+} \end{aligned} \Rightarrow$

$[K_{0.64}]^{+0.64} [R^{2+}_{2.85}R^{3+}_{0.15}]^{+0.15}_{3.00} [Al_{0.81}Si_{3.19}]^{-0.81}O_{10}(OH)_2$

$$
\begin{aligned}
& 0.15Ti^{4+} \quad (7) \\
+ & 0.74R^{3+} \\
& 0.16K^+
\end{aligned}
$$

Stable Ti-Free Biotite

The first reaction is almost the reverse of the reaction that produced metastable chlorite from allogenic biotite at the chlorite isograd, although the chemical variability of the products of the two reactions is distinctly different. The 2:1 octahedral sheet of the metastable Ti-chlorite, which was carried through from the same sheet of the allogenic biotite, is not preserved in the reaction at the biotite isograd. As noted above, this is consistent with the high degree of chemical exchange and structural reorganization of this reaction. In common with titaniferous allogenic biotite, the metastable Ti-biotite has a significant number of apparent octahedral vacancies. The Al produced during this reaction could be consumed by the nucleation of fine grained authigenic biotite in the sandstone pore spaces.

The reaction of metastable Ti-biotite to a coarse grained Ti-free biotite that is identical in composition with fine grained authigenic biotite occurs at the same temperature. This reaction, which removes the last of the metastable titaniferous mafic layer silicate phases observed in the geothermal system, produces a biotite with no vacancies, low interlayer occupancy, and a low octahedral Al content.

Many coarse grained chlorite analyses in the 1061–1067 m depth interval at temperatures near 315°C contain significant K, and optical examination of these grains indicates that these chlorites contain thin bands of biotite parallel to cleavage. When these analyses are plotted on a variation diagram the trends produced indicate that these thin bands consist of equilibrated low K, low Al and high Mg biotite, not allogenic biotite. Thus, at temperatures of approximately 10°C lower than the biotite isograd, trace amounts of authigenic biotite form in the micro-compositional environment of the coarse grained chlorite where a precursor mica-like lattice exists, but do not form away from chlorite where independent nucleation of biotite would be required.

Discussion

The conversion of a suite of allogenic layer silicate minerals to their authigenic equivalents in porous sandstone within the currently active Salton Sea Geothermal system was a complex process involving a number of apparently metastable intermediate phases. These metastable phases were produced within the geothermal system and at least partially equilibrated with that system, but reacted at varying rates to eventually produce authigenic minerals that were as equilibrated as possible within the time–temperature constraints of the evolving geothermal system. The apparent reaction rates of the allogenic layer silicates at temperatures near 190°C reflect, in inverse order, the stability ranges of their authigenic counterparts in the geothermal system. Biotite, which is not stable within the geothermal system for another 125°C, reacts very rapidly to either equilibrated chlorite or, for the most part, to a metastable titaniferous chlorite. Muscovite, which is not created by the prograde sequence from dioctahedral clay for another 90°C, reacts at a moderate rate such that it persists for some 65°C into the chlorite zone before it is completely replaced. Chlorite, which is stable in the geothermal system at 190°C, apparently reacts very little, as evidence of reaction of coarse grained allogenic chlorite, with normal optical properties, to fine grained authigenic chlorite, while observed, is very rare. The compositional overlap of allogenic and equilibrated chlorite is sufficient that little reaction is to be expected.

Investigation of the actual reactions strongly indicates that specific structural elements may be preserved intact in the product layer silicates, and that different lattice sites react at different rates and to different degrees. At temperatures near 190°C, the reaction of allogenic muscovite to mixed layer illite/smectite apparently occurs in two steps, producing a short-lived metastable phengitic phase with a domain structure as an intermediate reaction phase. In the first reaction step, little exchange occurs in the interlayer site while significant Si for Al exchange and Mg addition occur in the 2:1 layer. In the second step, in which the original muscovite structure is completely disrupted to form an aggregate of <0.005 mm grains, a sharp decrease in interlayer K occupancy to values typical of slightly expandable illite/smectite occurs. Expandable layers with exchangeable Mg are formed at this time. Illite/smectite after muscovite is similar to matrix illite/smectite except for a lower phengite content. At slightly higher temperatures, muscovite reacts directly to non-expandable illite.

The metastable titaniferous chlorite produced by reaction of allogenic biotite has the greatest range of persistence in the geothermal system of any of the metastable layer silicate phases. Chlorite replaced biotite directly on a layer-by-layer basis, and during this reaction the 2:1 octahedral sheet of the reactant biotite was apparently transferred intact to the product metastable chlorite. Stabilization of the 2:1 octahedral sheet was probably caused by the small, highly charged Ti^{4+} cation. The metastable chlorite thus took on anomalous biotite-like optical properties directly related to the Ti-content of the

2:1 octahedral sheet. The higher $Mg/(Fe+Mg)$ ratio of metastable chlorite relative to all other chlorites suggests that the newly created interlayer octahedral sheet was Mg-rich. Since other sites in the metastable chlorite were apparently free to react, the activation energy barrier responsible for persistence of the metastable chlorite is effectively equivalent to the energy necessary to remove Ti^{4+} from the specific sites it occupies in the 2:1 octahedral sheet. This energy barrier was sufficiently large that complete disruption of the 2:1 octahedral sheet did not occur until at interlayer deficient, siliceous biotite was itself stable within the geothermal system. Despite the complete exchange of the 2:1 octahedral sheet at the biotite isograd at 325°C, the product of reaction of the metastable chlorite was not the stable form of biotite, but was in part a completely recrystallized metastable titaniferous biotite. This metastable biotite reacted within 10°C of the biotite isograd to stable Ti-free authigenic biotite, implying that once the Ti-rich 2:1 octahedral sheet of the metastable chlorite was disrupted, all sites within the metastable biotite were reactive and reaction to the stable phase was relatively rapid.

The importance of structural factors is supported by the observation that the first authigenic biotite observed in the system is formed entirely within pre-existing grains of idioblastic, coarse grained equilibrated chlorite, at temperatures some 10 degrees lower than compositionally identical biotite is able to nucleate from the fluid phase. This emphasizes the sluggishness of many of these reactions as well as the importance of a preexisting lattice on which to form a presumably equilibrium mineral phase. Much of the compositional variability observed in low grade layer silicates appears due to the specific reaction that produced each grain. Those grains produced by replacement reactions appear to inherit at least some of the compositional characteristics of the reactant phase, and in some cases whole structural elements may be passed on intact. Thus in the geothermal system chlorites after biotite, chlorite, feldspar or dioctahedral layer silicate each may be compositionally distinct, and all different from chlorite nucleated directly from the fluid phase. The effects of structural control and replacement reaction variability appear to be more important in these very porous sandstones than effects due to variations in fluid chemistry in various micro environments. Once these various phases are formed, the intergrain compositional variability gradually decreases as reaction with the pervasive fluid phase continues with increasing temperature. This effect is reflected in the geothermal system by the large compositional variability of mixed layered illite/smectite at 190°C, the moderate variability of illite near 250°C, and the very restricted composition of authigenic muscovite at temperatures over 290°C. Authigenic chlorite shows considerable compositional variability throughout the calcite-chlorite zone, reflecting the apparent slow equilibration rate of chlorite. The variability of chlorite contrasts sharply with that of authigenic biotite,

most of which is the reaction product of chlorite breakdown and which shows very restricted compositional variability.

It is clear that the reaction among the various coarse grained layer silicates in the geothermal system is strongly dependent on kinetic factors, and must be considered in a site-by-site basis. The number of metastable phases produced and the variable rates of reaction observed indicate that great care must be taken in low temperature systems such as these in applying equilibrium thermochemical concepts to reactions in these systems. It is also clear that, in geothermal systems such as this in which time, temperature, and fluid compositions can be determined to reasonable degrees of reliability, it will be possible to eventually understand these complex reactions and to gain insight into the energetics of these reactions.

Acknowledgments

References

Brown, E. H. (1967) The greenschist facies in part of eastern Otago, New Zealand. Contributions to Mineralogy and Petrology, 14, 259–292.

Butler, B. C. M. (1967) Chemical study of minerals from the Moine Schists of the Ardnamurchen area, Argyllshire, Scotland. Journal of Petrology, 8, 233–267.

Chinner, G. A. (1960) Pelitic gneisses with varying ferrous/ferric ratios from Glen Clova, Angus, Scotland. Journal of Petrology, 1, 178–217.

Cooper, A. F. (1972) Progressive metamorphism of metabasic rocks from the Haast Schist Group of Southern New Zealand. Journal of Petrology, 13, 457–492.

Deer, W. A., Howie, R. A., and Zussman, J. (1962) Rock-Forming Minerals: Vol. 3. Sheet Silicates. Longmans, Green & Co., London.

Dodge, F. C. W., Smith, V. C., and Mays, R. E. (1969) Biotites from granitic rocks of the central Sierra Nevada Batholith, California. Journal of Petrology, 10, 250–270.

Guidotti, C. V., and Sassi, F. P. (1976) Muscovite as a petrogenetic indicator mineral in pelitic schists. Neues Jahrbuch für Mineralogie, Abhandlungen, 127, 97–142.

Helgeson, H. C. (1968) Geologic and thermodynamic characteristics of the Salton Sea geothermal system. American Journal of Science, 266, 129–166.

Hower, J., and Mowatt, T. C. (1966) The mineralogy of illites and mixed-layer illite/montmorillonites. The American Mineralogist, 51, 825–854.

Kendall, C. (1976) Petrology and stable isotope geochemistry of three wells in the Buttes area of the Salton Sea Geothermal Field, Imperial Valley, California. M.S. Thesis, University of California, Riverside, Institute of Geophysics and Planetary Physics Report No. 76/17, 211.

Lambert, R. St. J. (1959) The mineralogy and metamorphism of the Moine Schists of the Moran and Knoydant Districts of Invernes-shire. Transactions of the Royal Society of Edinburgh, 63(3), 533–588.

Lee, T. and Cohen, L. H. (1979) Onshore and offshore measurements of temperature gradients in the Salton Sea geothermal area, California. Geophysics, 44, 206–215.

Mather, J. D. (1970) The biotite isograd and the lower greenschist facies in the Dalradian rocks of Scotland. Journal of Petrology, 11, 254–276.

McDowell, S. D. and Elders, W. A. (1980) Authigenic layer silicate minerals in borehole Elmore 1, Salton Sea Geothermal Field, California, USA. Contributions to Mineralogy and Petrology, 74, 293–310.

McDowell, S. D., and McCurry, M. O. (1977) Active metamorphism in the Salton Sea Geothermal Field, California. Geological Society of America Abstracts with Programs, 9(7), 1088.

Millot, G. (1970) Geology of clays. Masson, et. cie., Paris.

Muffler, L. P. J., and Doe, B. (1968) Composition and mean age of detritus of the Colorado River in the Salton Trough, southeastern California. Journal of Sedimentary Petrology, 38, 384–399.

Muffler, L. P. J., and White, D. E. (1969) Active metamorphism of Upper Cenozoic sediments in the Salton Sea Geothermal Field and the Salton Trough, southeastern California. Geological Society of America Bulletin 80, 157–182.

Palmer, T. D. (1975) Characteristics of geothermal wells located in the Salton Sea Geothermal Field, Imperial Valley, California. University of California Lawrence Livermore Lab Report UCR-51976.

Randall, W. (1974) An analysis of the subsurface structure and stratigraphy of the Salton Sea Geothermal Anomaly, Imperial County, California. Ph.D. Thesis, University of California, Riverside.

Van de Kamp, P. C. (1973) Holocene continental sedimentation in the Salton Basin, California: A reconnaissance. Geological Society of America Bulletin, 84, 827–848.

Weaver, C. E. and Pollard, L. D. (1973) The chemistry of clay minerals. Developments in Sedimentology 15, Elsevier Scientific Publishing Company, Amsterdam.

Zen, E. (1959) Clay mineral-carbonate relations in sedimentary rocks. American Journal of Science, 257, 29–43.